

Development of an ischemic fracture healing model in mice

Maximilian M MENGER^{1,2}, Janine STUTZ^{1,3}, Sabrina EHNERT^{2,4}, Andreas K NUSSLER^{2,4}, Mika F ROLLMANN², Steven C HERATH², Benedikt J BRAUN², Tim POHLEMANN³, Michael D MENGER¹, and Tina HISTING²



¹ Institute for Clinical & Experimental Surgery, Saarland University, Homburg/Saar; ² Department of Trauma and Reconstructive Surgery, Eberhard Karls University Tübingen, BG Trauma Center Tübingen, Tübingen; ³ Department of Trauma, Hand and Reconstructive Surgery, Saarland University, Homburg/Saar; ⁴ Department of Trauma and Reconstructive Surgery, BG Trauma Center Tübingen, Siegfried Weller Institute for Trauma Research, Eberhard Karls University Tübingen, Tübingen, Germany
Correspondence: maximilian.menger@uks.eu
Submitted 2021-08-05. Accepted 2022-03-29.

Background and purpose — In fracture healing, ischemia caused by vascular injuries, chronic vascular diseases, and metabolic comorbidities is one of the major risk factors for delayed union and non-union formation. To gain novel insights into the molecular and cellular pathology of ischemic fracture healing, appropriate animal models are needed. Murine models are of particular interest, as they allow to study the molecular aspects of fracture healing due to the availability of both a large number of murine antibodies and gene-targeted animals. Thus, we present the development of an ischemic fracture healing model in mice.

Material and methods — After inducing a mild ischemia by double ligation of the deep femoral artery in CD-1 mice, the ipsilateral femur was fractured by a 3-point bending device and stabilized by screw osteosynthesis. In control animals, the femur was fractured and stabilized without the induction of ischemia. The femora were analyzed at 2 and 5 weeks after fracture healing by means of radiology, biomechanics, histology, and histomorphometry.

Results — The surgically induced ischemia delayed and impaired the process of fracture healing. This was indicated by a lower Goldberg score, decreased bending stiffness, and reduced bone callus formation in the ischemic animals when compared with the controls.

Interpretation — We introduce a novel ischemic femoral fracture healing model in mice, which is characterized by delayed bone healing. In future, the use of this model may allow both the elucidation of the molecular aspects of ischemic fracture healing and the study of novel treatment strategies.

Despite the increasing knowledge on the physiological basis of fracture healing, delayed unions and non-union formation remain a major clinical problem (1). There are a variety of comorbidities and risk factors that may contribute to the failure of fracture healing. Among these factors, an inadequate blood supply may represent a major determinant for healing failure (2).

In fact, previous work has demonstrated that half of patients suffering from vascular injuries experience complications in bone healing (2). This compares with the 10% non-union rate generally observed in fracture healing (1). Apart from acute vascular injuries, comorbidities such as peripheral arterial occlusive diseases (PAOD), diabetes, and smoking but also aging hamper bone regeneration by inhibiting angiogenesis and vascularization (3,4). The impaired blood supply results in ischemia, which leads to a shortage of oxygen and nutrients at the fracture site. This hypoxic environment causes cell death and delays chondrocyte and osteoblast differentiation, which both deteriorate the process of fracture healing (5). However, the exact cellular and molecular mechanisms are not completely understood.

To investigate the complex pathophysiology of fracture healing under ischemic conditions and to develop novel treatment strategies, appropriate animal models are needed (6). These animal models must be well standardized and must closely mimic the clinical situation in humans. In recent years, mice became of increasing interest in trauma research, because they allow the study of the molecular mechanisms of fracture healing due to the availability of a large number of antibodies and gene-targeted strains.

Therefore, we established a novel model of ischemic fracture healing in mice. Femoral mid-shaft fractures were sta-

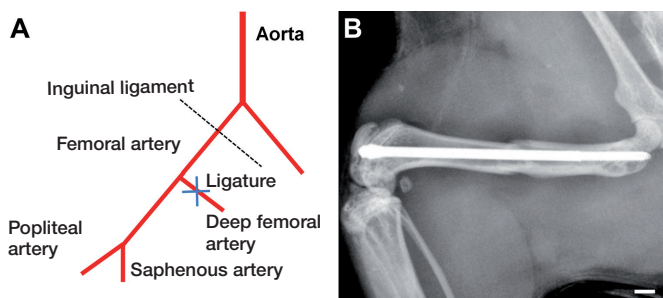


Figure 1. Schematic illustration of the surgically induced ischemia. The femoral artery was ligated between the inguinal ligament and the popliteal–saphenous bifurcation (A). Radiograph of a fractured mouse femur after the stabilization with a MouseScrew (B). Scale bar: 1.0 mm.

bilized by screw osteosynthesis (7) and moderate hind limb ischemia was induced by double ligation of the superficial femoral artery. Control animals received femoral mid-shaft fracture and screw osteosynthesis without the induction of ischemia. Fracture healing was then analyzed by radiographic, biomechanical, histological, and histomorphometric analyses. Because the mechanical stability at a late time point of fracture healing is of most clinical relevance, we have chosen the bending stiffness at 5 weeks after surgery as the parameter of primary interest and hypothesized that the detrimental effects of mild ischemia at the fracture site lead to reduced bending stiffness at 5 weeks after surgery.

Material and methods

Animals

28 CD-1 mice with a mean bodyweight of 30–40 g and an age of 12–16 weeks were used. The animals were housed at a 12-hour/12-hour light/dark cycle and had free access to tap water and standard pellet food (Altromin, Lage, Germany).

Surgical procedure

Mice were anesthetized by i.p. injection of xylazine (25 mg/kg BW) and ketamine (75 mg/kg BW). The stabilization of femur fractures was performed with the MouseScrew (RisSystems, Davos, Switzerland), allowing micromovements at the fracture site and, thus, endochondral healing (7). Under aseptic conditions a 6 mm medial parapatellar incision was performed at the right knee in the direction of the femoral artery. Mild hindlimb ischemia was induced by double ligation of the deep femoral artery distal of the inguinal ligament, using 6-0 synthetic sutures (Figure 1A) ($n = 14$). The patella was then dislocated laterally. At the intercondylar notch the intramedullary canal was opened using a drill bit (0.5 mm in diameter). Additionally, the greater trochanter was drilled retrogradely over the intramedullary cavity using an injection needle (0.4 mm in diameter). Then, a tungsten guide wire (0.2 mm in diameter) was inserted through the needle and the femur

was fractured by a 3-point bending device. Subsequently, the MouseScrew was inserted over the guide wire, resulting in a stable osteosynthesis achieved by interfragmentary compression through the screw. The screw consisted of a distal cone-shaped head (0.8 mm in diameter) and a proximal thread (M 0.5 mm, length 4 mm) allowing fracture compression. After fracture fixation, the patella was repositioned and the wound was closed using 6-0 synthetic sutures. Fracture and implant position were confirmed by radiography (Figure 1B). In control animals the same surgical procedure was performed, but without induction of ischemia ($n = 14$). Due to the high standardization of the model, no animals were lost to implant dislocation or anesthesia. The 2-week time point was chosen to analyze the early time point of fracture healing, whereas the 5-week time point was used to investigate the long-term healing outcome of femoral fractures. Of note, we observed a reliable femoral fracture consolidation at 5 weeks after surgery with the present model in previous studies (8,9).

Radiological analysis

At the end of the 2- ($n = 7$ each group) and 5- ($n = 7$ each group) week observation period the animals were re-anesthetized and lateral radiographs of the healing femora were performed. Fracture healing was classified according to Goldberg score, stage 0 indicating radiological non-union, stage 1: possible union, and stage 2: radiological union (10). The analysis was blinded in both groups.

Biomechanical analysis

For biomechanical analysis, the right and left femora were resected at 2 ($n = 7$ each group) and 5 ($n = 7$ each group) weeks after fracture and freed from soft tissue. After removing the implants, callus stiffness was measured with a non-destructive test using a 3-point bending device (MiniZwick Z 2.5; Zwick, Ulm, Germany). This allowed the use of specimens for additional histological and histomorphometrical analyses and, thus, reduction in the number of laboratory animals needed. Due to the different stages of healing, the loads that had to be applied varied markedly between the individual animals. Loading was stopped individually in every case when the actual load displacement curve deviated more than 1% from linearity. The analysis was blinded in both groups. To account for differences in bone stiffness of the individual animals, the unfractured left femora were also analyzed, serving as an internal control. All values of the fractured femora are given as absolute values and in percentage of the corresponding unfractured femora. The bending stiffness (N/mm) was calculated from the linear elastic part of the load-displacement diagram (11).

Histology and histomorphometry

7 bones from each group were analyzed at 2 and 5 weeks after fracture healing. Bones were fixed in IHC zinc fixative (BD Pharmingen, San Diego, CA) for 24 hours, decalcified in 13%

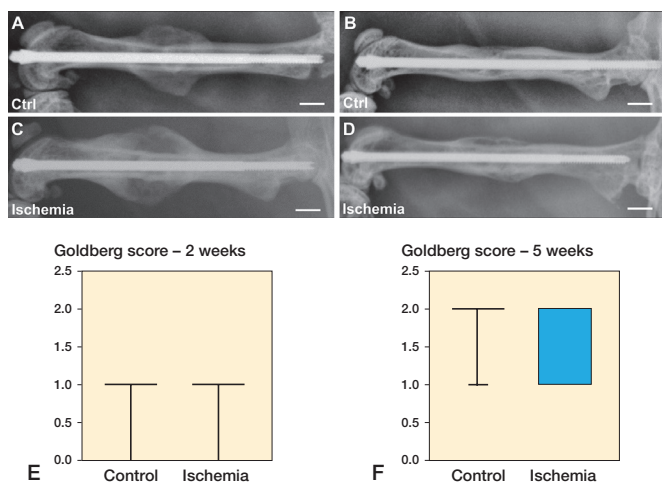


Figure 2. Radiological images of femora of control (A, B) and ischemic animals (C, D) at 2 weeks (A, C) and 5 (B, D) weeks after fracture healing. Scale bars: 2 mm. E, F: Goldberg score analyses at 2 weeks (E) and 5 weeks (F) after fracture healing in controls and ischemic animals. $p = 0.07$ vs. control.

EDTA solution for 2 weeks, and then embedded in paraffin. Longitudinal sections of $5 \mu\text{m}$ thickness were stained with Saffranin-O. With a $1.25\times$ lens and an Olympus BX60 microscope (Olympus, Tokyo, Japan), a Zeiss Axio Cam and Axio Vision system (version 3.1, Carl Zeiss, Oberkochen, Germany), and the ImageJ Analysis System (NIH, Bethesda, MD), structural indices were calculated according to the suggestions provided by Gerstenfeld et al. (12). These included total bone callus area (total osseous tissue area)/total callus area (TOTAr/CAR [%]), cartilaginous callus area/total callus area (CgAr/CAR [%]), and fibrous tissue callus area/total callus area (FTAr/CAR [%]). The analysis was blinded in both groups.

Statistics

For statistical analyses of data, medians and quartiles were calculated for each group per time point. Comparisons between the groups were performed by the exact version of the non-parametric Mann–Whitney U-test. All statistics were performed using the SigmaPlot 13.0 software (Jandel Corporation, San Rafael, CA, USA). A p -value of < 0.05 was considered significant.

Ethics, funding, and potential conflict of interest

All experiments were performed according to the German legislation on protection of animals and the National Institutes of Health (NIH) Guide for the Care and Use of Laboratory Animals (NIH Publications No. 8023, revised 1978, Institute of Laboratory Animal Resources, National Research Council, Washington, DC, USA). The experiments were approved by the local governmental animal protection committee (approval number: 24/2014). For this study no funding was received. The authors declare that they have no competing interests regarding this study.

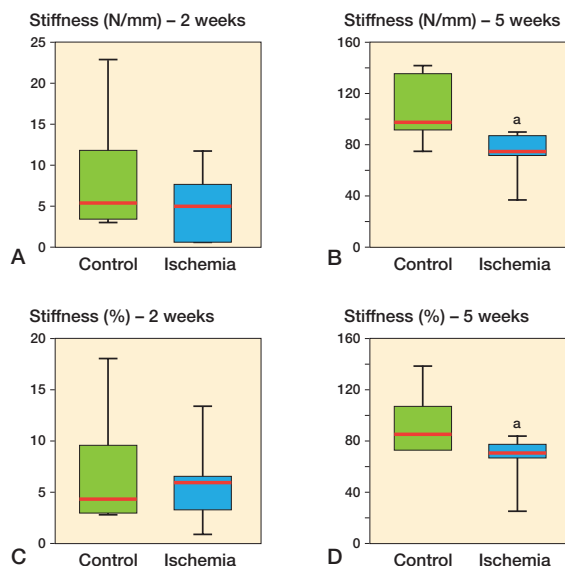


Figure 3. Biomechanical analysis of bending stiffness at 2 weeks (A, C) and 5 weeks (B, D) after fracture healing in controls and ischemic animals. Data is given in absolute values (N/mm) (A, B) and in percentage to the contralateral femora (%) (C, D). ^a $p < 0.05$ vs. control.

Results

Radiological analysis (Figure 2)

Radiological analysis showed typical signs of endochondral bone healing and osseous bridging at 2 and 5 weeks after fracture healing. The Goldberg score showed similar values between the 2 groups at 2 weeks after fracture healing. At 5 weeks after fracture healing a lower Goldberg score was observed in the ischemic animals when compared with controls ($p = 0.07$).

Biomechanical analysis (Figure 3)

Biomechanical analysis showed slightly lower bending stiffness at 2 weeks after fracture healing ($p = 0.7$ and $p = 0.9$) and lower bending stiffness at 5 weeks after fracture healing ($p = 0.004$ and $p = 0.03$) in the ischemia group when compared with the controls. Statistically significant differences between the ischemia and the control group at 5 weeks were found when comparing the absolute data as well as the relative (to unfractured contralateral bone) data.

Histology and histomorphometry (Figure 4)

Both groups showed signs of endochondral fracture healing with a typical distribution of cartilage tissue and woven bone in histological and histomorphometric analyses of callus and fracture zone, 2 weeks after healing. 5 weeks after fracture healing the cartilage and woven bone tissue was replaced by lamellar bone tissue reconstituting the normal anatomic and load-bearing properties of the femoral bone. Interestingly, we found a significantly increased amount of cartilage tissue

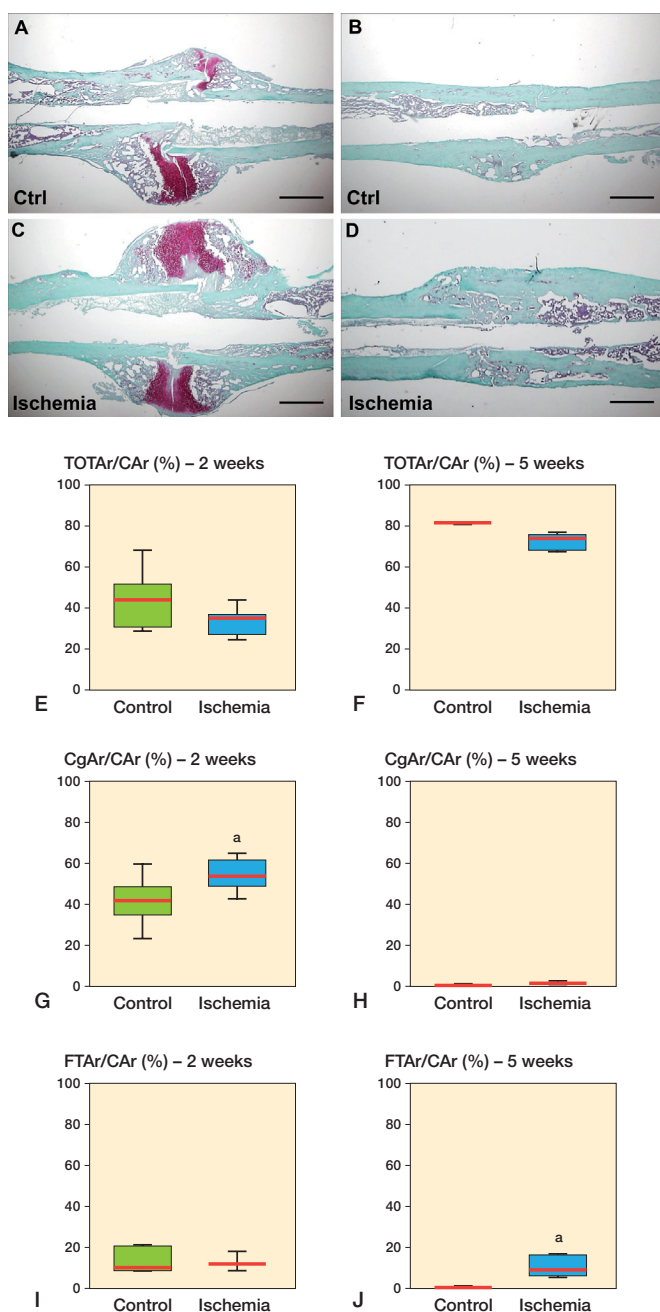


Figure 4. Representative histological images at 2 weeks (A, C) and 5 weeks after fracture healing (B, D) in controls (A, B) and ischemic animals (C, D). Scale bars: 1 mm. E–I: Histomorphometric analysis of the tissue distribution within the callus, including total osseous tissue callus area/total callus area (TOTAr/CAr (%)) (E, F), cartilaginous callus area/total callus area (CgAr/CAr [%]) (G, H), and fibrous tissue callus area/total callus area (FTAr/CAr [%]) (I, J) at 2 weeks (E, G, I) and 5 weeks (F, H, J) of fracture healing in controls and ischemic animals. ^a $p < 0.05$ vs. control.

(54% [SD 7.4] vs. 42% [12], $p = 0.03$) and a markedly reduced amount of bone tissue (33% [6.8] vs. 45% [13], $p = 0.05$) in the ischemia group at 2 weeks after fracture healing. The amount of fibrous tissue (13% [3.1] vs. 13% [5.7]) was comparable in

both groups at 2 weeks after fracture healing. After 5 weeks the amount of bone tissue (88% [4.8] vs. 99% [0.9], $p = 0.003$) was lower in the ischemia group, whereas the ratio of remnant fibrous tissue (11% [5.1] vs. 0.3% [0.3], $p = 0.003$) was enhanced. The amount of remnant cartilage tissue at 5 weeks after fracture healing (1.4% [0.6] vs. 0.6% [0.6], $p = 0.07$) did not differ statistically significant between the 2 groups.

Discussion

We developed a novel model of ischemic fracture healing in mice and tested the hypothesis that the mild ischemic environment (13,14) induced by the ligation of the femoral artery results in reduced bending stiffness at 5 weeks after surgery. Our experiments confirmed our hypothesis. The reduced bending stiffness in the ischemic animals observed at 5 weeks after surgery was associated with a decreased Goldberg score, delayed callus remodeling, and a lesser amount of bone tissue, indicating an impaired and delayed process of fracture healing.

Ischemia caused by physical injuries, metabolic comorbidities, and chronic ischemic diseases represents a major risk factor for complications in fracture healing (15). In order to prevent delayed union or non-union formation, further insights into the molecular and cellular basis of ischemic fracture healing are necessary. Therefore, animal models are needed to mimic the human situation of pathological bone healing. Only with the use of such models can the effectiveness of novel treatment approaches be analyzed. In recent years, mice have become of increasing interest in biomedical research. This is due to (i) low husbandry costs, (ii) a short reproductive cycle, (iii) the broad availability of transgenic strains, and (iv) the large number of monoclonal antibodies (15).

Lu et al. (5) developed a murine model of surgically induced ischemic fracture healing. This model involved the resection of the femoral artery between the inguinal ligament and the saphenous/popliteal bifurcation and was followed by a closed transverse mid-diaphyseal tibia fracture. The induced ischemia resulted in multiple defects in bone repair, including impaired cell differentiation and survival, an increase in fibrous and adipose tissue at the fracture site, and an overall reduced callus area resulting in incomplete fracture bridging. The resection of the femoral artery created severe ischemia in the affected tissue (14). However, many metabolic conditions, such as peripheral arterial occlusive disease or diabetes, do not generate an abrupt and fulminant ischemia, but rather create a hypoxic environment in a slow and gradual manner over time (3,16). Moreover, even severe trauma-induced blood vessel injuries are usually addressed by emergency surgery to reestablish the blood supply and to prevent the development of critical ischemia, which may lead to the loss of the entire limb (17,18). However, the ligation of the femoral artery below the inguinal ligament, as performed in our study, results in only

mild ischemia (14). This moderate ischemic environment may mimic the pathophysiology of ischemic fracture healing in humans more accurately than a severe or fulminant ischemia, which, thus, may be a major advantage of the presented model here. In addition, the stabilization of the fracture by an external fixator, as suggested in the model of Lu et al. (5), may be rather time-consuming and impractical in experimental applications. However, the intramedullary fixation used in the present study does not only represent a more feasible and sophisticated technique of osteosynthesis, but is also the clinical standard.

Another experimental model by Oetgen et al. (19) uses the cauterization of the lateral periosteum at the femoral fracture site to achieve a partial disruption of the blood supply. The authors found reliable non-union formation 63 days after surgery with no signs of bony bridging in mice with periosteal cauterization (19). However, this approach rather mimics the extensive soft tissue damage often associated with open fractures, than an ischemia caused by metabolic comorbidities. Moreover, the authors clearly state that the fracture fixation by an intramedullary gauge needle provides no axial or rotational stability, which may have also contributed to non-union formation (19). Thus, the study of Oetgen et al. (19) introduces a model of non-union formation caused by periosteal cauterization and non-stable fracture fixation. In contrast, in our study no additional tissue damage was induced by periosteal cauterization and biomechanical instability could be avoided by fracture stabilization with the MouseScrew. Thus, the delayed fracture healing observed in the present study is solely induced by the mild ischemia after the ligation of the deep femoral artery.

Bone regeneration is a complex and strictly organized process that occurs in a sequentially orchestrated manner of inflammation, mesenchymal stem cell condensation, chondrogenesis, angiogenesis, and osteogenesis (20). The development of the soft callus tissue is followed by a remodeling process, which involves the resorption of cartilaginous tissue and the replacement of woven to lamellar bone (8). Interestingly, we found an increased amount of cartilaginous tissue at 2 weeks after fracture healing in the ischemic animals compared with the controls. This may be explained by the fact that hypoxia induces chondrocyte differentiation (21,22) and, thus, favors the differentiation of chondrocytes rather than osteoblasts. This hypothesis is supported by an *in vitro* study of Murphy and Polak (23), which revealed that chondrogenesis of articular chondrocytes proceeds much more effectively in cultures that have reduced oxygen levels. Hence, ischemia may delay the process of callus remodeling by promoting chondrogenesis, thereby decelerating the resorption of cartilaginous tissue. Moreover, we found a reduced amount of bone tissue and an increased amount of fibrous tissue at 5 weeks after fracture within the callus tissue of the ischemic animals. These findings are in line with the results of Lu et al. (5), who found fibrous tissue at the fracture site at later stages of bone healing

in the ischemic animals. Thus, it is likely that ischemia, on the one hand, caused a suppression of osteogenesis and, on the other hand, induced fibrogenic proliferation and differentiation, resulting in the formation of fibrous tissue in place of bone tissue. It is well established that fibrous tissue is abundant within the callus of non-unions in both animal models and humans (6,24,25). Hence, ischemia does not only delay the process of bone regeneration but may also induce non-union formation.

In summary, we developed a novel murine model of ischemic bone regeneration, which results in delayed and impaired fracture healing. While there is a clear association between impaired blood supply and reduced bone healing, experimental studies that investigate treatment strategies under ischemic conditions are still lacking. Strategies that promote and facilitate bone regeneration, such as the delivery of growth factors (26) and tissue engineering approaches (27), have been mostly explored in non-compromised bone injury models (15). The present mouse model, however, may overcome this problem. Such a murine model not only offers the possibility of molecular analysis, but also allows the investigation of a great number of animals in a short period of time (6). Thus, further studies with this model will be helpful to enlarge our understanding of ischemic fracture healing, as well as to evaluate and compare different treatment strategies.

MMM: data analysis, figure preparation, and manuscript writing. JS: surgery, radiological, biomechanical, and histological analysis. SE, AN, MFR, SCH, BJB, TP: data discussion and interpretation, critical manuscript revision. MDM: idea and study design, data interpretation, manuscript writing. TH: idea and study design, data discussion and interpretation, critical manuscript revision.

The authors are grateful for the excellent technical assistance of Janine Becker.

Acta thanks Henrik Eckardt and Ulrik Kähler Olesen for help with peer review of this study.

1. **Einhorn T A, Gerstenfeld L C.** Fracture healing: mechanisms and interventions. *Nat Rev Rheumatol* 2015; 11(1): 45-54. doi: 10.1038/nrrheum.2014.164.
2. **Dickson K F, Katzman S, Paiement G.** The importance of the blood supply in the healing of tibial fractures. *Contemp Orthop* 1995; 30(6): 489-93.
3. **Jiao H, Xiao E, Graves D T.** Diabetes and its effect on bone and fracture healing. *Curr Osteoporos Rep* 2015; 13(5): 327-35. doi: 10.1007/s11914-015-0286-8.
4. **Hernigou J, Schuind F.** Smoking as a predictor of negative outcome in diaphyseal fracture healing. *Int Orthop* 2013; 37(5): 883-7. doi: 10.1007/s00264-013-1809-5.
5. **Lu C, Miclau T, Hu D, Marcucio R S.** Ischemia leads to delayed union during fracture healing: a mouse model. *J Orthop Res* 2007; 25(1): 51-61. doi: 10.1002/jor.20264.
6. **Garcia P, Holstein J H, Maier S, Schaumloffel H, Al-Marrawi F, Hannig M, et al.** Development of a reliable non-union model in mice. *J Surg Res* 2008; 147(1): 84-91. doi: 10.1016/j.jss.2007.09.013.

7. **Holstein J H, Matthys R, Histing T, Becker S C, Fiedler M, Garcia P, et al.** Development of a stable closed femoral fracture model in mice. *J Surg Res* 2009; 153(1): 71-5. doi: 10.1016/j.jss.2008.02.042.
8. **Histing T, Stenger D, Scheuer C, Metzger W, Garcia P, Holstein J H, et al.** Pantoprazole, a proton pump inhibitor, delays fracture healing in mice. *Calcif Tissue Int* 2012; 90(6): 507-14. doi: 10.1007/s00223-012-9601-x.
9. **Menger M M, Merscher B, Scheuer C, Braun B J, Herath S C, Rollmann M F, et al.** Amlodipine accelerates bone healing in a stable closed femoral fracture model in mice. *Eur Cell Mater* 2021; 41: 592-602. doi: 10.22203/eCM.v041a38.
10. **Goldberg V M, Powell A, Shaffer J W, Zika J, Bos G D, Heiple K G.** Bone grafting: role of histocompatibility in transplantation. *J Orthop Res* 1985; 3(4): 389-404. doi: 10.1002/jor.1100030401.
11. **Histing T, Garcia P, Matthys R, Leidinger M, Holstein J H, Kristen A, et al.** An internal locking plate to study intramembranous bone healing in a mouse femur fracture model. *J Orthop Res* 2010; 28(3): 397-402. doi: 10.1002/jor.21008.
12. **Gerstenfeld L C, Wronski T J, Hollinger J O, Einhorn T A.** Application of histomorphometric methods to the study of bone repair. *J Bone Miner Res* 2005; 20(10): 1715-22. doi: 10.1359/JBMR.050702.
13. **Stabile E, Kinnaird T, la Sala A, Hanson S K, Watkins C, Campia U, et al.** CD8+ T lymphocytes regulate the arteriogenic response to ischemia by infiltrating the site of collateral vessel development and recruiting CD4+ mononuclear cells through the expression of interleukin-16. *Circulation* 2006; 113(1): 118-24. doi: 10.1161/CIRCULATIONAHA.105.576702.
14. **Tang G, Charo D N, Wang R, Charo I F, Messina L.** CCR2^{-/-} knock-out mice revascularize normally in response to severe hindlimb ischemia. *J Vasc Surg* 2004; 40(4): 786-95. doi: 10.1016/j.jvs.2004.07.012.
15. **Haffner-Luntzer M, Hankenson K D, Ignatius A, Pfeifer R, Khader B A, Hildebrand F, et al.** Review of animal models of comorbidities in fracture-healing research. *J Orthop Res* 2019; 37(12): 2491-8. doi: 10.1002/jor.24454.
16. **Conte S M, Vale P R.** Peripheral arterial disease. *Heart Lung Circ* 2018; 27(4): 427-32. doi: 10.1016/j.hlc.2017.10.014.
17. **Kinlay S.** Management of critical limb ischemia. *Circ Cardiovasc Interv* 2016; 9(2): e001946. doi: 10.1161/CIRCINTERVENTIONS.115.001946.
18. **Farber A, Eberhardt R T.** The current state of critical limb ischemia: a systematic review. *JAMA Surg* 2016; 151(11): 1070-1077. doi: 10.1001/jamasurg.2016.2018.
19. **Oetgen M E, Merrell G A, Troiano N W, Horowitz M C, Kacena M A.** Development of a femoral non-union model in the mouse. *Injury* 2008; 39(10): 1119-26. doi: 10.1016/j.injury.2008.04.008.
20. **Holstein J H, Menger M D, Scheuer C, Meier C, Culemann U, Wirbel R J, et al.** Erythropoietin (EPO): EPO-receptor signaling improves early endochondral ossification and mechanical strength in fracture healing. *Life Sci* 2007; 80(10): 893-900. doi: 10.1016/j.lfs.2006.11.023.
21. **Bassett C A, Herrmann I.** Influence of oxygen concentration and mechanical factors on differentiation of connective tissues in vitro. *Nature* 1961; 190: 460-1. doi: 10.1038/190460a0.
22. **Miclau K R, Brazina S A, Bahney C S, Hankenson K D, Hunt T K, Marcucio R S, et al.** Stimulating fracture healing in ischemic environments: does oxygen direct stem cell fate during fracture healing? *Front Cell Dev Biol* 2017; 5: 45. doi: 10.3389/fcell.2017.00045.
23. **Murphy C L, Polak J M.** Control of human articular chondrocyte differentiation by reduced oxygen tension. *J Cell Physiol* 2004; 199(3): 451-9. doi: 10.1002/jcp.10481.
24. **Choi P, Ogilvie C, Thompson Z, Miclau T, Helms J A.** Cellular and molecular characterization of a murine non-union model. *J Orthop Res* 2004; 22(5): 1100-7. doi: 10.1016/j.orthres.2004.03.008.
25. **Reed A A, Joyner C J, Brownlow H C, Simpson A H.** Human atrophic fracture non-unions are not avascular. *J Orthop Res* 2002; 20(3): 593-9. doi: 10.1016/S0736-0266(01)00142-5.
26. **Orth M, Shenar A K, Scheuer C, Braun B J, Herath S C, Holstein J H, et al.** VEGF-loaded mineral-coated microparticles improve bone repair and are associated with increased expression of epo and RUNX-2 in murine non-unions. *J Orthop Res* 2019; 37(4): 821-31. doi: 10.1002/jor.24267.
27. **Romero R, Travers J K, Asbury E, Pennybaker A, Chubb L, Rose R, et al.** Combined delivery of FGF-2, TGF-beta1, and adipose-derived stem cells from an engineered periosteum to a critical-sized mouse femur defect. *J Biomed Mater Res A* 2017; 105(3): 900-11. doi: 10.1002/jbm.a.35965.